

SHOCK ADIABATS AND THE NEAR ZONE IN AN EXPLOSION IN A DRILLING MUD

Yu. P. Nelasov

UDC 622.235.6

Shock adiabats have been determined for drilling muds of various densities, and the effects of the muds on the near zone in an explosion are examined.

A drilling mud is a colloidal system consisting of particles of clay and a material that increases the density as well as small amounts of surface-active substances, which are mixed with water or petroleum. The characteristic dimensions of the particles are 10–1000 Å [1], so from the viewpoint of mechanics of continuous media it may be considered as a homogeneous liquid whose density is determined in the main by the content of the density-increasing agent. The viscosity of the solution is dependent on the particle size and the nature of the base liquid, and it may vary from 40 to 200–400 cP. In practice, drilling muds are frequently made up from locally available materials, so we made studies with a model solution based on water, bentonite clay, an alkaline reagent, and fly ash as the density-increasing agent. The basic parameters that were controlled were the density and the viscosity, which were determined by standard methods. Tables can be employed to convert from centipoise to seconds in the funnel method of measurement.

Figure 1 shows the scheme used to measure the shock adiabats. The mean wave and mass velocities of the shock waves were measured from the transit time over present baselines, the times of arrival of the shock waves and of the material from the free surface being recorded from the arrival of light in thin air slots.

Figure 1 shows that the explosive charge, which produces a planar shock wave, lies under the Lucite plate A, with a cylindrical recess 1 for the drilling mud, which is 18 mm in diameter and 3–4 mm deep. This block is built up from individual sheets of known thickness in such a way as to leave a slot of thickness 0.1 mm at the edge, which serves to check the shape of the front and to test for the arrival of the shock wave in the drilling mud. Additional blocks of Lucite B and C are attached to the base of block A at distances of 0.1 and 3–4 mm from the surface of the drilling mud, which indicate the instant of arrival of the shock wave from the solution and the instant of arrival of the detached layer of solution at the end of the measuring baseline. Block C is covered with aluminum foil of thickness 0.1 mm, which forms with block C an air slot of thickness 0.1 mm, which serves to cut off the illumination from the air shock wave. Mirror 2 is used to turn the beam. Item 3 in Fig. 1 represents a high-speed camera, and Fig. 2 shows a typical time recording of the process, where t_1 is the time of propagation of the shock wave in the solution, while t_2 is the total time of motion of the solution to the end of the measuring baseline. The accuracy of measurement of the baselines was ± 0.1 mm, while the intensity of the shock wave was adjusted via the density and composition of the explosive, and also by replacing the lower part of block A by an aluminum disk of thickness 2.5 mm.

Figure 3 and Table 1 give the results, the densities of the muds being given on the curves. The figure also shows the shock adiabats of Lucite I and water II. It is clear from Fig. 3 that the effective rigidity of the drilling solution increases substantially with the density. The shock adiabats of the drilling muds can be represented in the form $D=A+Bu$, where D is the wave velocity in km/sec and u is the mass velocity (Table 2 and Fig. 4). For muds of density from 1.30 to 2.17 g/cm³, the spread in the experimental values does not exceed 5%, but the limits of error rose to 10% for 1.07 g/cm³.

Moscow. Translated from Zhurnal Prikladnoi Mekhaniki i Tekhnicheskoi Fiziki, No. 3, pp. 77–82, May–June, 1973. Original article submitted August 29, 1972.

© 1975 Plenum Publishing Corporation, 227 West 17th Street, New York, N.Y. 10011. No part of this publication may be reproduced, stored in a retrieval system, or transmitted, in any form or by any means, electronic, mechanical, photocopying, microfilming, recording or otherwise, without written permission of the publisher. A copy of this article is available from the publisher for \$15.00.

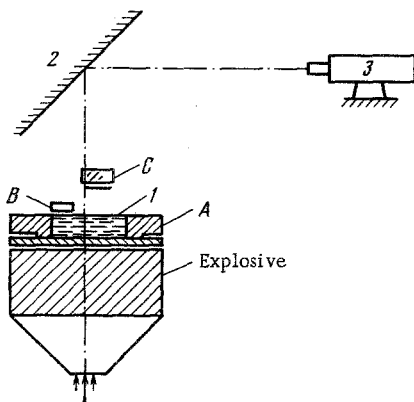


Fig. 1

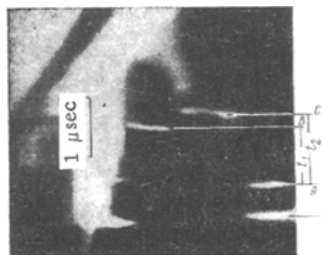


Fig. 2

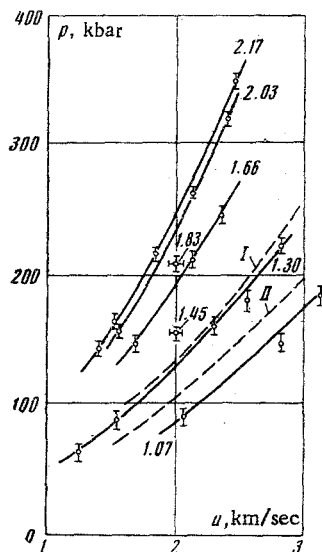


Fig. 3

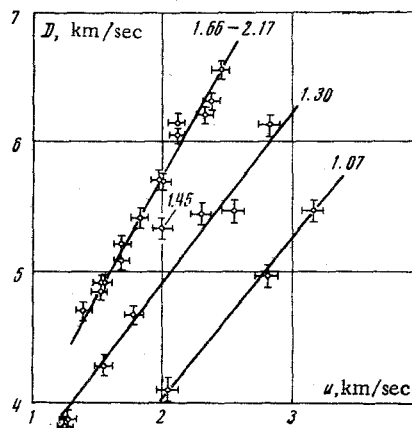


Fig. 4



Fig. 5

The shock adiabats of the muds are almost identical in D - u coordinates for the density range 1.66 to 2.17 g/cm^3 ; the dynamic rigidity of the solutions falls at lower densities, and the adiabat for a clay suspension without density-increasing agent is below that for water when the density is 1.07 g/cm^3 .

To perform approximate calculations from the composition of the mud, it is best to calculate the shock adiabat from the generalized one [2], as for homogeneous liquid, and the initial velocity of sound may be calculated from the additive compressibility of the components. Table 3 gives the density and speed of sound for the basic components of the muds, the contents of the other components being small and therefore negligible in approximate calculations. Rougher estimates may be made by using the actual density of the mud together with $D=1.67+1.81 u$, which is suitable for water [3, 4]. The possible discrepancy between such calculations and observed values does not exceed 15% in p - u coordinates.

It is important to know how the intensity of the shock waves varies directly adjacent to the charge when the surrounding liquid density varies. An autoclave fitted with optical windows was used in experiments to measure the speed of shock waves in water in the near zone of an explosion using spherical charges and hydrostatic pressures from 1 to 960 kgf/cm^2 ; the spherical charge of PETN was covered with one or two layers of epoxide resin and was initiated from the center by a small amount of lead azide; this lay on the axis of the autoclave, and the propagation pattern of the shock waves was recorded with an SFR camera

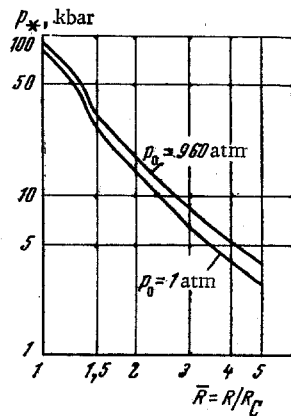


Fig. 6

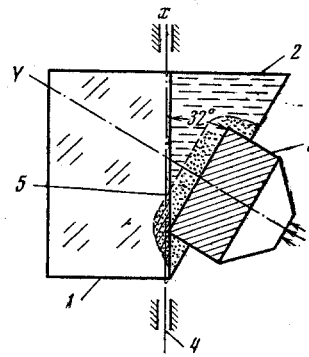


Fig. 7

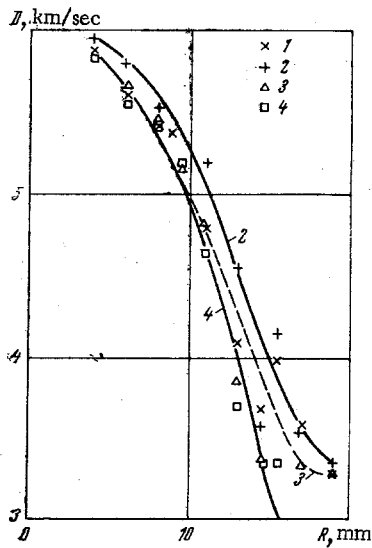


Fig. 8

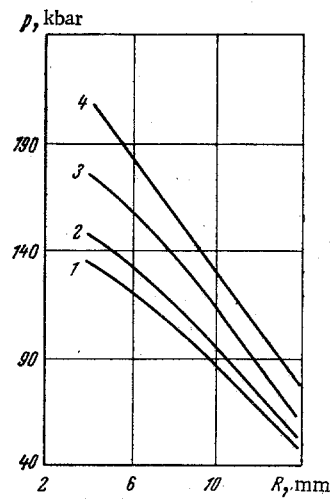


Fig. 9

(Fig. 5), with a scale of 1:2-2.5. The resulting time patterns were measured with a BMI-1 microscope to give an accuracy of wave velocity measurement of 2.5-3%, and these gave the velocity of the shock wave as a function of distance from the center of the charge for various hydrostatic pressures.

The peak wave pressures were derived from the equation of state for water [4] and data on the compressibility [5], which were used to calculate the shock adiabats for water for various initial pressures. The following are working formulas for the high peak pressure region [4]:

$$p_* - p_0 = d(\rho_*^k - \rho_0^k) \\ D_*^2 = (p_* - p_0)/[\rho_0(1 - \rho_0/\rho_*)]; \quad u_*^2 = (p_* - p_0)/\rho_0(1 - \rho_0/\rho_*) \quad (1)$$

where $d=4250$, $k=6.29$, p is the pressure in kgf/cm^2 , ρ is density in g/cm^3 , D is the wave velocity, and u is the mass speed. Subscript 0 refers to the initial conditions, while an asterisk relates to values at the shock-wave front. A preliminary analysis showed that k is practically independent of the initial pressure, so only ρ_0 is dependent on the initial pressure in (1). Table 4 gives the shock adiabats for water for three initial pressures.

Figure 6 shows the peak pressure in the shock wave at the front as a function of distance from the center of the charge, which has been constructed via the above-wave adiabats for water for two initial pressures; it is clear that this is suitable for spherical PETN charges of diameter more than 8 mm out to distances $\bar{R} = R/R_c = 5$; when the initial pressure varies from 1 to 960 kgf/cm^2 , which corresponds to a density change in water of 4.4%, the curve shifts upwards by 10%. There is a characteristic kink in the curve

TABLE 1

ρ_0 , g/cm ³	u , m/sec	D , m/sec	p_0 , kbar	ρ_0 , g/cm ³	u , m/sec	D , m/sec	p_0 , kbar
2.17	1396	4706	142.0	1.66	1690	5220	146.5
	2450	6560	349		2110	6050	211.0
	1530	4915	163.2		2315	6380	245
2.032	1840	5420	216.1	1.45	2000	5330	154.5
	2110	6150	263	1.362	1780	4670	110
	2380	6313	320	1.32	1547	4280	87.4
	1560	4920	156	1.250	1250	3810	62.8
1.924	1979	5710	217.5	1.29	2820	6130	223
	1690	5090	166	2300	5440	161.2	
1.83	1995	5700	208	1.30	2555	5470	181.2
	2330	6220	263	1260	3870	63.5	
1.78	1530	4850	125	1.07	2810	4980	147
				3175	5480	185	
				2050	4106	90.3	

TABLE 2

ρ_0 , g/cm ³	A , km/sec	B	Press. range, kbar
1.07	1.50	1.25	до 185
1.30	2.27	1.33	до 230
1.66+2.17	2.0	1.88	125-300

TABLE 3

Substances	ρ_0 , g/cm ³	c_0 , km/sec
Water at 20° C	1.0	1.490
Bentonite clay	2.1	2.30
Flue dust	4.5	5.0

TABLE 4

p_0 , kgf/cm ²	T_0 , °C	ρ_0 , g/cm ³	A , km/sec	B
1	20	1.00	1.67	1.81
500	20	1.024	1.89	1.61
1000	20	1.044	2.14	1.60

near $\bar{R} = 1.4$, but on the whole the trend in the peak pressure with distance is the same for all the pressures, and the decay of the amplitude in the shock wave with distance determines the rate of change of pressure behind the shock wave front [6]; thus, one can assume that the characteristic time of action for the pressure behind the shock-wave front in the near zone is practically independent of the hydrostatic pressure and the initial density of the water in the range examined.

In these experiments, the density of the liquid varies only slightly, and subsequently the tests were done with drilling muds, which are opaque; thus, to estimate the effects of the density on the shock-wave propagation, we used a method illustrated in Fig. 7. The explosive charge 3 was set at 32° to the surface of the Lucite block 1, and this produced a planar shock wave. The space between the explosive charge and block 1 was filled with the mud 2, and after decimation detonation of the charge 3, the SFR camera (4 is the camera slot and 5 is the shock-wave front) recorded the moments of emergence of the shock-wave front from the solution into the Lucite. As the geometry was known, the resulting time pattern enables one to determine the velocity of propagation as a function of distance, and the previously recorded shock adiabats enable one to determine the peak pressure at the front and to obtain a pattern for the decay of the planar shock wave in the drilling mud. Figures 8 and 9 show the results, and it is clear that the peak pressure is approximately proportional to the density of the drilling mud, whereas the velocity of propagation is almost independent of the density. The points numbered 1-4 in Fig. 8 relate to densities ρ of 1.21, 1.39, 1.56, and 1.72 g/cm³, respectively.

Similar relationships were obtained with charges of more complicated configuration (cylindrical charges with curved shock waves entering the mud), and these qualitatively confirmed the above results. With a given geometry, the intensity of the shock waves increased with the density of the solution; the decline in the velocity of propagation with distance was almost exactly the same in all cases, so the characteristic time of action of the pressure behind the shock-wave front did not alter substantially; here, one can assume that the specific momentum conveyed by the shock wave in the near zone should increase roughly in proportion to the initial density of the mud.

Other measurements showed that variation of the viscosity from 40 cP to the point of complete structure formation did not influence the propagation and amplitude of the shock wave out to 6-7 times the radius of the explosive charge.

LITERATURE CITED

1. A. K. Miskarli, Colloid Chemistry of Clay Drilling Suspensions [in Russian], Azerneshr, Baku (1963).
2. V. M. Gogolev, V. G. Myrkin, and G. I. Yablokova, "An approximate equation of state for a solid," Zh. Prikl. Mekh. i Tekh. Fiz., No. 5 (1963).
3. R. Cole, Underwater Explosions [Russian translation], Izd. IL, Moscow (1950).
4. Yu. S. Yakovlev, Explosion Hydrodynamics [in Russian], Sudpromgiz, Moscow and Leningrad (1961).
5. G. Tamman, Ad. Rührenbeck Ann. der Physik, Vol. 13, H-1-8 (1932), p. 69.
6. V. N. Kostyuchenko, "Shock-wave parameters in water near a spherical explosive charge", Zh. Prikl. Mekh. i Tekh. Fiz., No. 2 (1961).